

International Journal of Modern Physics D
© World Scientific Publishing Company

The property difference between the neutron star PSR J0348+0432 and its proto neutron star

Xian-Feng Zhao^{1,2}

¹*School of Sciences, Southwest Petroleum University, Chengdu, 610500 China*

²*School of Electronic and Electrical Engineering, Chuzhou University, Chuzhou, 239000, China
zhaopioneer.student@sina.com*

Received Nov 21, 2016

Revised Day Month Year

Communicated by Managing Editor

The property difference between the neutron star PSR J0348+0432 and its proto neutron star is studied in the framework of the relativistic mean field theory considering neutrino trapping. We see that the central baryon number density of the proto neutron star PSR J0348+0432 is in the range $\rho_{c,PNS} = 0.539 \sim 0.698 \text{ fm}^{-3}$, which is smaller than that of the neutron star PSR J0348+0432 $\rho_{c,NS} = 0.634 \sim 0.859 \text{ fm}^{-3}$. Inside the neutron star PSR J0348+0432, only the neutrons, protons, Λ and Ξ^- produce, whereas the hyperons $\Sigma^-, \Sigma^0, \Sigma^+$ and Ξ^0 all do not appear. But in the proto neutron star PSR J0348+0432, hyperons $\Sigma^-, \Sigma^0, \Sigma^+$ and Ξ^0 all will produce, though their relative particle number density are still very small, no more than 2%. This shows that higher temperature will be advantageous to the hyperon production.

Keywords: nucleon coupling constants; relativistic mean field theory; proto neutron star.

1. Introduction

In the supernova, core implosion will take 0.5~1.0 s and within a few milliseconds the lepton-rich core will settle into hydrostatic equilibrium. Thus, a proto neutron star (PNS) produces. Only after tens of seconds, it will change into a neutron star (NS). For a PNS with $M=1.4 M_{\odot}$, within $t=0\sim 20$ s, its temperature T changes from 30 MeV to 5 MeV ¹.

The phase diagram at sub-saturation densities is strongly affected by the electromagnetic interaction, though it is almost independent of the electric charge at supra-saturation density ². Although the PNS has strong magnetic field, but its effect on the dynamics is found to be mild ³. The symmetry energy plays a dramatic role in determining the structure of NSs and the evolution of core-collapsing supernovae ⁴. And at the end of the evolution, an isolated NS has a certain maximum value of mass, which it can not reach ⁵.

Within the finite-temperature Brueckner-Bethe-Goldstone many-body theory, the research results show that neutrino trapping will shift the appearance of hyperons to larger baryon density and will stiffen considerably the equation of state ^{6,7}.

2 *Xian-Feng Zhao*

Recent years, two massive NSs have been discovered one after another. In 2010, the NS PSR J1614-2230 was observed by Demorest et al ⁸ and the other more massive NS PSR J0348+0432, whose mass is $M=2.01\pm 0.04 M_{\odot}$ and is almost the largest one by far, was also found by Antoniadis et al in 2013 ⁹. The research results show that a non-linear relativistic mean field (RMF) model, which is consistent with up-to-date semi-empirical nuclear and hypernuclear data, can allow for neutron stars with hyperon cores and $M > 2 M_{\odot}$. This model involves hidden-strangeness scalar and vector mesons, coupled only to hyperons, and quartic terms involving vector meson fields ¹⁰.

The mass of the massive NS/PNS is very large and this will no doubt limit the NS/PNS's properties, such as the field strength of mesons, chemical potentials of baryons, particle distribution and the NS/PNS's mass and radius.

For the massive PNSs, their properties are very important for the understanding of the stellar evolution. The PNS has higher temperature compared to the NS and therefore its properties must be different from those of its corresponding NS. About this case, we have greater interest.

For finite temperatures above 1 MeV, the neutrino mean free path in neutron star matter is less than the radius of the star so that neutrinos are trapped and have to be taken into account in the beta-equilibrium. So the calculations for the proto-neutron star case should be done for conserved lepton number ¹¹.

In this paper, we use the RMF theory to study the property difference between the NS PSR J0348+0432 and its PNS with neutrino trapping being considered.

2. The RMF theory

Under the RMF approximation, the Lagrangian density of hadron matter considering the mesons $f_0(975)$ (denoted as σ^*) and $\phi(1020)$ (denoted as ϕ) reads as follows ^{12,13}

$$\begin{aligned} \mathcal{L} = & \sum_B \bar{\Psi}_B (i\gamma_{\mu}\partial^{\mu} - m_B + g_{\sigma B}\sigma + g_{\sigma^* B}\sigma^* - g_{\omega B}\gamma^0\omega - g_{\phi B}\gamma^0\phi - g_{\rho B}\gamma^0\tau_3\rho)\Psi_B \\ & - \frac{1}{2}m_{\sigma}^2\sigma^2 - \frac{1}{3}g_2\sigma^3 - \frac{1}{4}g_3\sigma^4 + \frac{1}{2}m_{\omega}^2\omega^2 + \frac{1}{2}m_{\rho}^2\rho^2 - \frac{1}{2}m_{\sigma^*}^2\sigma^{*2} + \frac{1}{2}m_{\phi}^2\phi^2 \\ & + \sum_{\lambda=e,\mu} \bar{\Psi}_{\lambda} (i\gamma_{\mu}\partial^{\mu} - m_{\lambda})\Psi_{\lambda}. \end{aligned} \quad (1)$$

For the PNS matter considering neutrino trapping, the partition function of baryon reads as

$$\ln Z_B = \frac{V}{T} \langle \mathcal{L} \rangle + \sum_B \frac{2J_B + 1}{2\pi^2} \int_0^{\infty} k^2 dk \left\{ \ln \left[1 + e^{-(\varepsilon_B(k) - \mu_B)/T} \right] \right\} \quad (2)$$

From above we can obtain the total baryon number density, the energy density and the pressure as follows ^{14,15,16}

The property difference between the neutron star PSR J0348+0432 and its proto neutron star 3

$$\rho = \sum_B \frac{2J_B + 1}{2\pi^2} b_B \int_0^\infty k^2 n_B(k) dk, \quad (3)$$

$$\begin{aligned} \varepsilon = & \frac{1}{2} m_\sigma^2 \sigma^2 + \frac{1}{2} m_{\sigma^*}^2 \sigma^{*2} + \frac{1}{3} g_2 \sigma^3 + \frac{1}{4} g_3 \sigma^4 + \frac{1}{2} m_\omega^2 \omega_0^2 + \frac{1}{2} m_\phi^2 \phi^2 + \frac{1}{2} m_\rho^2 \rho_{03}^2 \\ & + \sum_B \frac{2J_B + 1}{2\pi^2} \int_0^\infty \kappa^2 n_B(k) d\kappa \sqrt{\kappa^2 + m_B^{*2}}, \end{aligned} \quad (4)$$

$$\begin{aligned} p = & -\frac{1}{2} m_\sigma^2 \sigma^2 - \frac{1}{2} m_{\sigma^*}^2 \sigma^{*2} - \frac{1}{3} g_2 \sigma^3 - \frac{1}{4} g_3 \sigma^4 + \frac{1}{2} m_\omega^2 \omega_0^2 + \frac{1}{2} m_\phi^2 \phi^2 + \frac{1}{2} m_\rho^2 \rho_{03}^2 \\ & + \frac{1}{3} \sum_B \frac{2J_B + 1}{2\pi^2} \int_0^\infty \frac{\kappa^4}{\sqrt{\kappa^2 + m_B^{*2}}} n_B(k) d\kappa, \end{aligned} \quad (5)$$

where, $n_B(k)$ is the Fermi-Dirac partition function of baryon

$$n_B(k) = \frac{1}{1 + \exp[(\varepsilon_B(k) - \mu_B)/T]}. \quad (6)$$

For the leptons, their interactions can be ignored at finite temperature and therefore their partition function read as

$$\begin{aligned} \ln Z_L = & \frac{V}{T} \sum_i \frac{\mu_i^4}{24\pi^2} \left[1 + 2 \left(\frac{\pi T}{\mu_i} \right)^2 + \frac{7}{15} \left(\frac{\pi T}{\mu_i} \right)^4 \right] \\ & + V \sum_\lambda \frac{1}{\pi^2} \int_0^\infty k^2 dk \left\{ \ln \left[1 + e^{-(\varepsilon_\lambda(k) - \mu_\lambda)/T} \right] \right\}, \end{aligned} \quad (7)$$

the first line represents the contribution of massless neutrinos and the second line the contribution of electrons and μ .

From above we can obtain the lepton number density and the contribution to the energy density and the pressure

$$\rho_l = \frac{1}{\pi^2} \int_0^\infty k^2 n_l(k) dk, \quad (8)$$

$$\rho_\nu = \frac{\pi^2 T^2 \mu_\nu + \mu_\nu^3}{6\pi^2}, \quad (9)$$

$$\varepsilon = \sum_l \frac{1}{\pi^2} \int_0^\infty \kappa^2 n_l(k) d\kappa \sqrt{\kappa^2 + m_l^2} = \sum_\nu \left(\frac{7\pi^2 T^4}{120} + \frac{T^2 \mu_\nu^2}{4} + \frac{\mu_\nu^4}{8\pi^2} \right), \quad (10)$$

$$p = \frac{1}{3} \sum_l \frac{1}{\pi^2} \int_0^\infty \frac{\kappa^4}{\sqrt{\kappa^2 + m_l^2}} n_l(k) d\kappa = \sum_\nu \frac{1}{360} \left(7\pi^2 T^4 + 30T^2 \mu_\nu^2 + \frac{15\mu_\nu^4}{\pi^2} \right) \quad (11)$$

The chemical potentials of baryons can be written as

4 *Xian-Feng Zhao*

$$\mu_i = \mu_n - q_i (\mu_e - \mu_{\nu e}). \quad (12)$$

To describe the neutrino trapping, we can define the content of lepton in PNS as

$$Y_{l\nu} = Y_l + Y_{\nu l} = \frac{\rho_l + \rho_{\nu l}}{\rho}. \quad (13)$$

For the NS, the RMF theory can be seen in Ref [13].

We use the Tolman-Oppenheimer-Volkoff (TOV) equation to obtain the mass and the radius of a NS/PNS ^{17,18}

$$\frac{dp}{dr} = -\frac{(p + \varepsilon)(M + 4\pi r^3 p)}{r(r - 2M)}, \quad (14)$$

$$M = 4\pi \int_0^R \varepsilon r^2 dr. \quad (15)$$

Here, the upper integration limit R is the radius of the star which contains the accumulated total mass M .

3. The parameters

In this work, the nucleon coupling constant is chosen as the GL85 set ¹⁹: the saturation density $\rho_0=0.145 \text{ fm}^{-3}$, binding energy $B/A=15.95 \text{ MeV}$, a compression modulus $K = 285 \text{ MeV}$, charge symmetry coefficient $a_{sym}=36.8 \text{ MeV}$ and the effective mass $m^*/m=0.77$.

We define the ratios of hyperon coupling constants to nucleon coupling constants as follows: $x_{\sigma h} = \frac{g_{\sigma h}}{g_\sigma}$, $x_{\omega h} = \frac{g_{\omega h}}{g_\omega}$, $x_{\rho h} = \frac{g_{\rho h}}{g_\rho}$, with h denoting hyperons Λ, Σ and Ξ .

According to SU(6) symmetry, $x_{\rho\Lambda} = 0, x_{\rho\Sigma} = 2, x_{\rho\Xi} = 1$ are selected ²⁰. The experimental data show that the hyperon well depth are $U_\Lambda^{(N)} = -30 \text{ MeV}$ ²¹, $U_\Sigma^{(N)} = 10 \sim 40 \text{ MeV}$ ^{22,23,24,25} and $U_\Xi^{(N)} = -18 \text{ MeV}$ ²⁶, respectively. Therefore, we choose $U_\Lambda^{(N)} = -30 \text{ MeV}$, $U_\Sigma^{(N)} = +30 \text{ MeV}$ and $U_\Xi^{(N)} = -18 \text{ MeV}$ in this work.

The calculating results show that the ratio of hyperon coupling constant to nucleon coupling constant is in the range of $\sim 1/3$ to 1 ²⁷. So in this work we choose $x_{\sigma\Lambda}=0.4, 0.5, 0.6, 0.7, 0.8, 0.9$ at first and the hyperon coupling constants $x_{\omega\Lambda}$ can be obtained by considering the restriction of the hyperon well depth [?]

$$U_h^{(N)} = m_n \left(\frac{m_n^*}{m_n} - 1 \right) x_{\sigma h} + \left(\frac{g_\omega}{m_\omega} \right)^2 \rho_0 x_{\omega h}. \quad (16)$$

Using the same method, $x_{\sigma\Sigma}$, $x_{\omega\Sigma}$, $x_{\sigma\Xi}$ and $x_{\omega\Xi}$ can be obtained (see Table 1).

The coupling constants of the mesons $f_0(975)$ and $\phi(1020)$ are $g_{\phi\Xi} = 2g_{\phi\Lambda} = -2\sqrt{2}g_\omega/3$ and $g_{f_0\Lambda}/g_\sigma = g_{f_0\Sigma}/g_\sigma = 0.69, g_{f_0\Xi}/g_\sigma = 1.25$, respectively ¹².

The property difference between the neutron star PSR J0348+0432 and its proto neutron star 5

Table 1. The hyperon coupling constants fitting to the experimental data of the well depth, which are $U_{\Lambda}^{(N)} = -30$ MeV, $U_{\Sigma}^{(N)} = +30$ MeV and $U_{\Xi}^{(N)} = -18$ MeV, respectively.

$x_{\sigma\Lambda}$	$x_{\omega\Lambda}$	$x_{\sigma\Sigma}$	$x_{\omega\Sigma}$	$x_{\sigma\Xi}$	$x_{\omega\Xi}$
0.4	0.3681	0.4	0.7597	0.4	0.4464
0.5	0.5090	0.5	0.9007	0.5	0.5874
0.6	0.6500			0.6	0.7284
0.7	0.7910			0.7	0.8693
0.8	0.9320				

In this work, the entropy per baryon is chosen as $S=2$. The content of lepton in PNS is chosen as $Y_{l\mu}=0$ and $Y_{le}=0.1$, respectively.

From Table 1, we can combine into 40 sets of parameters (see Table 2).

For each set of parameters in Table 2, we calculate the mass of the NS/PNS (see Fig. 1).

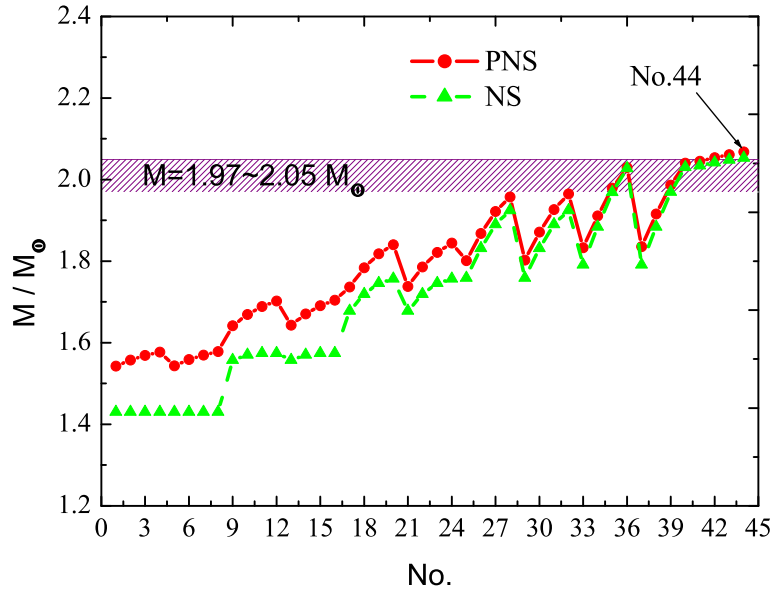


Fig. 1. The mass as a function of the parameters numbers.

We find that the maximum mass of the NS calculated by parameters 01 to 40 are all less than $2.05 M_{\odot}$. Then we further choose $x_{\sigma\Xi}=0.71, 0.73, 0.75, 0.77$, respectively. Thus, we obtain parameters 41 to 44 (see Table 2), by which the

6 *Xian-Feng Zhao*Table 2. The 44 sets of hyperon coupling constants used in this work and the corresponding NS/PNS's maximum mass claculated. The unit of the mass M is the solar mass M_{\odot} .

NO.	$x_{\sigma\Lambda}$	$x_{\omega\Lambda}$	$x_{\sigma\Sigma}$	$x_{\omega\Sigma}$	$x_{\sigma\Xi}$	$x_{\omega\Xi}$	$M_{max,PNS}$	$M_{max,NS}$
01	0.4	0.3681	0.4	0.7597	0.4	0.4464	1.5427	1.4300
02	0.4	0.3681	0.4	0.7597	0.5	0.5874	1.5577	1.4303
03	0.4	0.3681	0.4	0.7597	0.6	0.7284	1.5690	1.4303
04	0.4	0.3681	0.4	0.7597	0.7	0.8693	1.5771	1.4303
05	0.4	0.3681	0.5	0.9007	0.4	0.4464	1.5434	1.4300
06	0.4	0.3681	0.5	0.9007	0.5	0.5874	1.5586	1.4303
07	0.4	0.3681	0.5	0.9007	0.6	0.7284	1.5700	1.4303
08	0.4	0.3681	0.5	0.9007	0.7	0.8693	1.5783	1.4303
09	0.5	0.5090	0.4	0.7597	0.4	0.4464	1.6420	1.5576
10	0.5	0.5090	0.4	0.7597	0.5	0.5874	1.6691	1.5705
11	0.5	0.5090	0.4	0.7597	0.6	0.7284	1.6888	1.5746
12	0.5	0.5090	0.4	0.7597	0.7	0.8693	1.7021	1.5747
13	0.5	0.5090	0.5	0.9007	0.4	0.4464	1.6430	1.5576
14	0.5	0.5090	0.5	0.9007	0.5	0.5874	1.6705	1.5705
15	0.5	0.5090	0.5	0.9007	0.6	0.7284	1.6907	1.5746
16	0.5	0.5090	0.5	0.9007	0.7	0.8693	1.7045	1.5747
17	0.6	0.6500	0.4	0.7597	0.4	0.4464	1.7368	1.6780
18	0.6	0.6500	0.4	0.7597	0.5	0.5874	1.7838	1.7189
19	0.6	0.6500	0.4	0.7597	0.6	0.7284	1.8182	1.7460
20	0.6	0.6500	0.4	0.7597	0.7	0.8693	1.8403	1.7570
21	0.6	0.6500	0.5	0.9007	0.4	0.4464	1.7382	1.6780
22	0.6	0.6500	0.5	0.9007	0.5	0.5874	1.7860	1.7189
23	0.6	0.6500	0.5	0.9007	0.6	0.7284	1.8215	1.7460
24	0.6	0.6500	0.5	0.9007	0.7	0.8693	1.8447	1.7570
25	0.7	0.7910	0.4	0.7597	0.4	0.4464	1.8011	1.7590
26	0.7	0.7910	0.4	0.7597	0.5	0.5874	1.8683	1.8318
27	0.7	0.7910	0.4	0.7597	0.6	0.7284	1.9217	1.8904
28	0.7	0.7910	0.4	0.7597	0.7	0.8693	1.9579	1.9249
29	0.7	0.7910	0.5	0.9007	0.4	0.4464	1.8030	1.7590
30	0.7	0.7910	0.5	0.9007	0.5	0.5874	1.8714	1.8318
31	0.7	0.7910	0.5	0.9007	0.6	0.7284	1.9268	1.8904
32	0.7	0.7910	0.5	0.9007	0.7	0.8693	1.9652	1.9249
33	0.8	0.9320	0.4	0.7597	0.4	0.4464	1.8329	1.7911
34	0.8	0.9320	0.4	0.7597	0.5	0.5874	1.9114	1.8845
35	0.8	0.9320	0.4	0.7597	0.6	0.7284	1.9791	1.9690
36	0.8	0.9320	0.4	0.7597	0.7	0.8693	2.0297	2.0275
37	0.8	0.9320	0.5	0.9007	0.4	0.4464	1.8354	1.7911
38	0.8	0.9320	0.5	0.9007	0.5	0.5874	1.9156	1.8845
39	0.8	0.9320	0.5	0.9007	0.6	0.7284	1.9863	1.9694
40	0.8	0.9320	0.5	0.9007	0.7	0.8693	2.0407	2.0300
41	0.8	0.9320	0.5	0.9007	0.71	0.8834	2.0452	2.0343
42	0.8	0.9320	0.5	0.9007	0.73	0.9116	2.0536	2.0419
43	0.8	0.9320	0.5	0.9007	0.75	0.9398	2.0612	2.0483
44	0.8	0.9320	0.5	0.9007	0.77	0.9680	2.0682	2.0535

maximum masses obtained are also listed in Table 2. We see that parameter 44 can give the maximum mass greater than $2.05 M_{\odot}$. Therefore, we use parameter 44 to describe the properties of the NS/PNS PSR J0348+0432.

The property difference between the neutron star PSR J0348+0432 and its proto neutron star 7

4. The field strength of mesons σ , ω and ρ

Our calculations show that the central baryon number density of the NS PSR J0348+0432 is $\rho_{Bc,NS}=0.634\sim 0.859 \text{ fm}^{-3}$ and that of the PNS PSR J0348+0432 is $\rho_{Bc,PNS}=0.539\sim 0.698 \text{ fm}^{-3}$ (see Table 3).

Table 3. The results of the NS/PNS PSR J0348+0432 calculated in this work. The unit of the following physical quantities are: $M\sim M_{\odot}$; $\rho_c\sim \text{fm}^{-3}$; $\sigma_0, \omega_0, \rho_{03}\sim \text{fm}^{-1}$; $\mu_{nc}, \mu_{ec}\sim \text{fm}^{-1}$, respectively.

	NS PSR J0348+0432	PNS PSR J0348+0432
M	1.97~2.05	1.97~2.05
ρ_{Bc}	0.634~0.859	0.539~0.698
σ_c	0.321~0.366	0.290~0.326
ω_c	0.367~0.492	0.311~0.401
ρ_c	0.087~0.091	0.079~0.079
μ_{nc}	6.957~7.906	6.395~7.046
μ_{ec}	1.314~1.294	1.057~1.142
ρ_{nc}/ρ	64.3~48.3%	60.9~52.1%
ρ_{pc}/ρ	21.3~21.4%	17.6~18.7%
$\rho_{\Lambda c}/\rho$	14.4~23.8%	13.5~17.6%
$\rho_{\Sigma^- c}/\rho$	0~0%	0.06%~0.1%
$\rho_{\Sigma^0 c}/\rho$	0~0%	0.2%~0.4%
$\rho_{\Sigma^+ c}/\rho$	0~0%	0.8~1.4%
$\rho_{\Xi^- c}/\rho$	0~6.5%	6.3~8.4%
$\rho_{\Xi^0 c}/\rho$	0~0%	0.7~1.2%
ρ_{ec}/ρ	12.1~8.5%	10.3~10.1%
$\rho_{\mu c}/\rho$	9.2~6.4%	1.8~1.5%

The field strengths of mesons σ , ω and ρ as a function of the baryon number density are shown in Fig. 2. The thick lines show the central field strengths.

We see that the field strengths of mesons σ in the PNS PSR J0348+0432 are less than those in the NS PSR J0348+0432. At the center, the field strength of mesons σ of the PNS PSR J0348+0432 is in the range $\sigma_{PNSc}=0.290\sim 0.326 \text{ fm}^{-1}$, which is slightly smaller than that of the NS PSR J0348+0432 (in the range $\sigma_{NSc}=0.321\sim 0.366 \text{ fm}^{-1}$).

The field strength of mesons ω in the PNS PSR J0348+0432 and that in the NS PSR J0348+0432 make little difference corresponding to a same baryon number density ρ . But the central field strength of mesons ω of the NS PSR J0348+0432 is in the range $\omega_{NSc}=0.367\sim 0.492 \text{ fm}^{-1}$, while that of the PNS PSR J0348+0432 decreases to the range $\omega_{PNSc}=0.311\sim 0.401 \text{ fm}^{-1}$.

We also see that there are little differences between the field strength of meson ρ of the PNS PSR J0348+0432 and that of the NS PSR J0348+0432 corresponding to a same baryon number density ρ . In the center, the field strength of mesons ρ of the PNS PSR J0348+0432 is $\rho_{PNSc}=0.079 \text{ fm}^{-1}$, while that of the NS PSR J0348+0432 is in the range $\rho_{NSc}=0.087\sim 0.091 \text{ fm}^{-1}$.

From the above we see that the field strengths of mesons σ, ω and ρ of the PNS

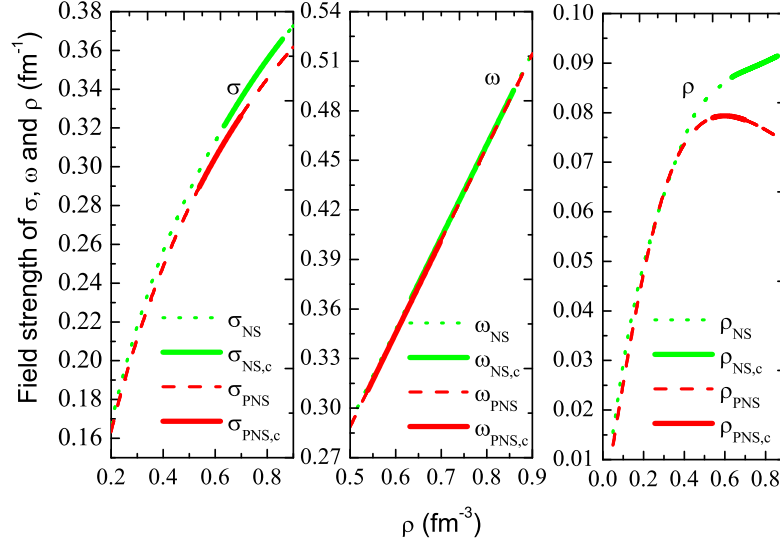


Fig. 2. The field strength of mesons σ , ω and ρ as a function of the baryon number density.

PSR J0348+0432 and those in the NS PSR J0348+0432 all make little differences corresponding to a same baryon number density ρ . But the value range of the central field strength of mesons σ , ω and ρ in the PNS PSR J0348+0432 is smaller than those in the NS PSR J0348+0432.

The central field strengths of mesons σ , ω and ρ also can be seen in Table 3.

5. The chemical potentials of neutrons and electrons

The chemical potentials of neutrons and electrons as a function of baryon number density are shown in Fig. 3. The thick lines show the central chemical potentials. We see the chemical potentials of neutrons of the PNS PSR J0348+0432 are less than those of the NS PSR J0348+0432 corresponding to a same baryon number density ρ . As $\rho < 0.18 \text{ fm}^{-3}$ the chemical potentials of electrons of the PNS PSR J0348+0432 are greater than those of the NS PSR J0348+0432 but are less than the latter as $\rho > 0.18 \text{ fm}^{-3}$.

The central chemical potential of neutrons of the PNS PSR J0348+0432 is in the range $\mu_{nc,PNS}=6.395\sim 7.046 \text{ fm}^{-1}$, while that of the NS PSR J0348+0432 is in the range $\mu_{nc,NS}=6.957\sim 7.906 \text{ fm}^{-1}$. The central chemical potential of electrons of the PNS PSR J0348+0432 is in the range $\mu_{ec,PNS}=1.057\sim 1.142 \text{ fm}^{-1}$, while that of the NS PSR J0348+0432 is in the range $\mu_{ec,NS}=1.314\sim 1.294 \text{ fm}^{-1}$.

The property difference between the neutron star PSR J0348+0432 and its proto neutron star 9

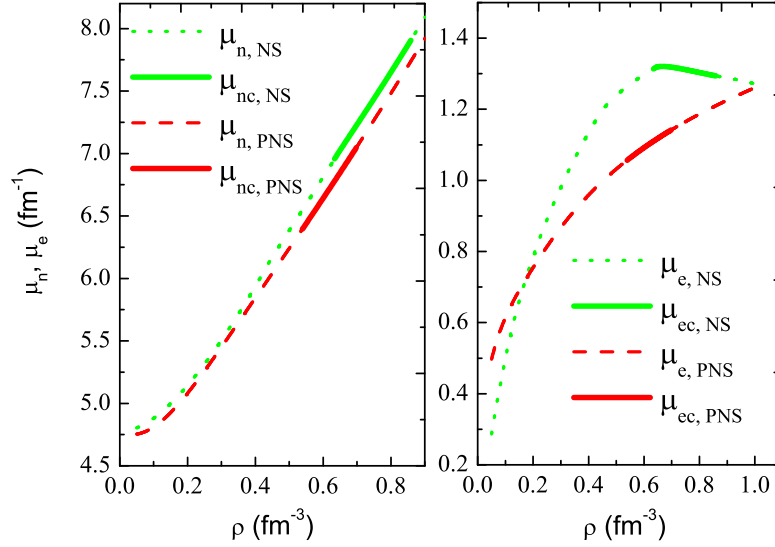


Fig. 3. The chemical potentials of neutrons μ_n and electrons μ_e as a function of baryon number density.

6. The relative particle number density of the baryons in the NS/PNS PSR J0348+0432

6.1. n , p , Λ

Figure 4 gives the relative particle number density ρ_i/ρ of neutrons, protons, Λ , electrons and μ s as a function of baryon number density ρ .

We see the relative particle number density of neutrons ρ_n/ρ in the PNS PSR J0348+0432 is less than those in the NS PSR J0348+0432 corresponding to a same baryon number density ρ . The relative particle number density of protons ρ_p/ρ in the PNS PSR J0348+0432 is greater than those in the NS PSR J0348+0432 as $\rho < 0.2083 \text{ fm}^{-3}$ but is less than the latter as $\rho > 0.2083 \text{ fm}^{-3}$. The relative particle number density of Λ ρ_Λ/ρ in the PNS PSR J0348+0432 is greater than that in the NS PSR J0348+0432.

The central relative particle number density of neutrons of the PNS PSR J0348+0432 is in the range $\rho_{nc,PNS}/\rho=60.9\sim 52.1\%$, while that of the NS PSR J0348+0432 is in the range $\rho_{nc,NS}/\rho=64.3\sim 48.3\%$.

The relative particle number density of protons at the center of the PNS PSR J0348+0432 is in the range $\rho_{pc,PNS}/\rho=17.6\sim 18.7\%$, while that of the NS PSR J0348+0432 is in the range $\rho_{pc,NS}/\rho=21.3\sim 21.4\%$.

The relative particle number density of Λ s at the center of the PNS PSR J0348+0432 is in the range $\rho_{\Lambda c,PNS}/\rho=13.5\sim 17.6\%$, while that of the NS PSR

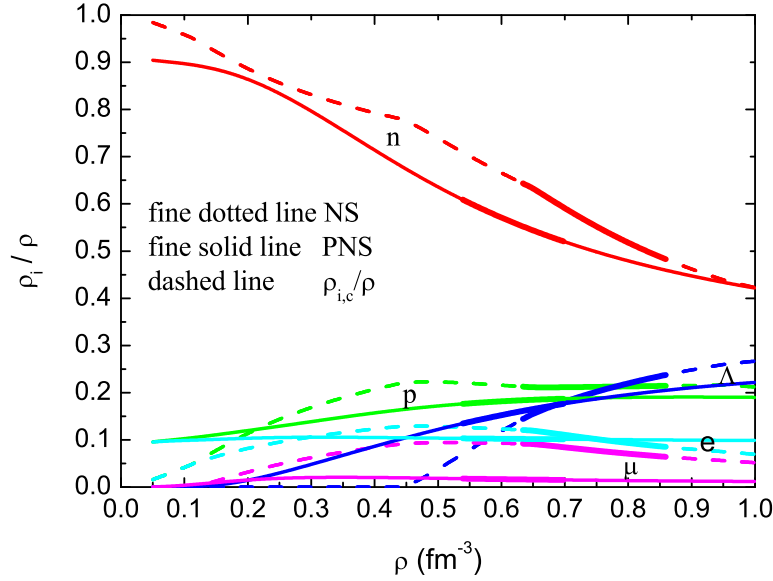


Fig. 4. The relative particle number density of n , p , Λ , e and μ as a function of baryon number density.

J0348+0432 is in the range $\rho_{\Lambda c, NS}/\rho=14.4\sim 23.8\%$.

From the above we see that the central relative number density of neutrons and protons in the PNS PSR J0348+0432 are all less than those in the NS PSR J0348+0432.

6.2. Σ^- , Σ^0 , Σ^+

In the NS PSR J0348+0432, the hyperons Σ^- , Σ^0 and Σ^+ all do not produce. But in the PNS PSR J0348+0432, they will all produce, though their relative particle number density are still very small, only less than 2%.

This means that although the positive well depth $U_{\Sigma}^{(N)}$ restricts the production of the Σ ^{28,29}, but the higher temperature will be advantageous to its production.

The relative particle number density of hyperon Σ as a function of baryon number density ρ is shown in Fig. 5.

6.3. Ξ^- , Ξ^0

The relative particle number density of Ξ^- and Ξ^0 as a function of baryon number density are shown in Fig 6.

We see that hyperons Ξ^- and Ξ^0 all will produce in the PNS PSR J0348+0432 whereas in the NS PSR J0348+0432 only Ξ^- appears. The central relative

The property difference between the neutron star PSR J0348+0432 and its proto neutron star 11

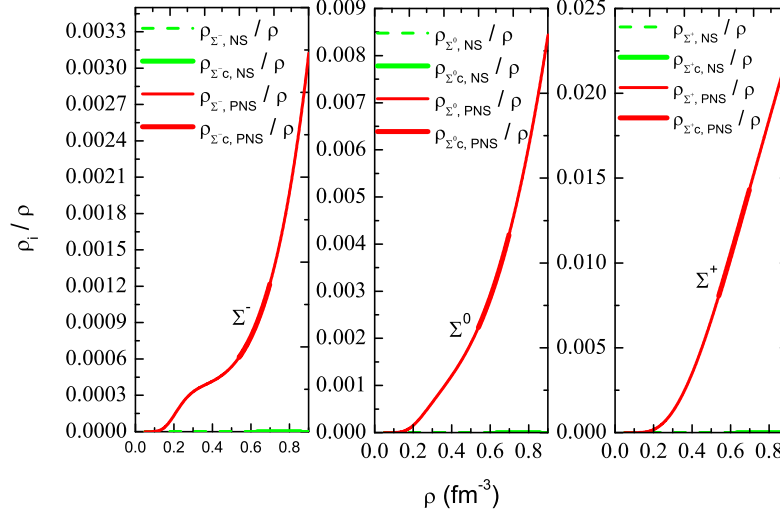


Fig. 5. The relative particle number density of Σ as a function of baryon number density.

particle number density of Ξ^- s in the NS PSR J0348+0432 is in the range $\rho_{\Xi^-,NS}/\rho=0\sim 6.5\%$, while that in the PNS PSR J0348+0432 is in the larger range $\rho_{\Xi^-,PNS}/\rho=6.3\sim 8.4\%$. Higher temperature will be advantageous to the production of hyperon Ξ^- .

In the NS PSR J0348+0432, the hyperons Ξ^0 do not produce. But in the PNS PSR J0348+0432 it produces, though the relative particle number density is still very small. In the center, the relative particle number density is only $\rho_{\Xi^0,PNS}/\rho=0.7\%\sim 1.2\%$, namely less than 2%.

7. Effect of temperature on the relative particle number density of the baryons in the PNS PSR J0348+0432

Effect of temperature on the relative particle number density of the baryons in the PNS PSR J0348+0432 is shown in Fig. 7. We see that the central temperature of the PNS PSR J0348+0432 is in the range $T_{c,PNS}=41.662\sim 45.685$ MeV corresponding to the relative particle number density of the baryons in the center $\rho_{c,PNS}=0.539\sim 0.698$ fm $^{-3}$.

From Fig. 7 we also see that the relative particle number density of neutrons decreases whereas those of p, Λ , Σ^- , Σ^0 , Σ^+ , Ξ^- and Ξ^0 all increase with the increase of the temperature.

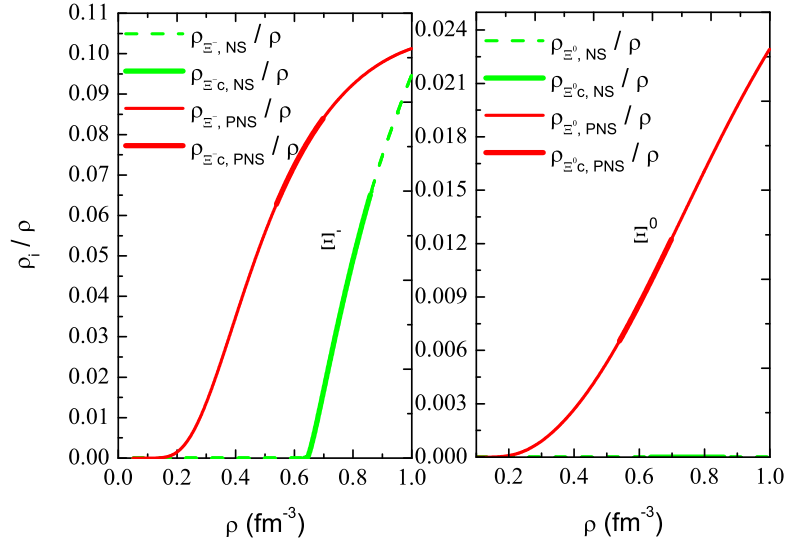


Fig. 6. The relative particle number density of Ξ^- and Ξ^0 as a function of baryon number density.

8. Conclusions

In this paper, we apply the RMF theory to study the property difference between the NS PSR J0348+0432 and its PNS. The entropy per baryon is selected as $S=2$.

We find that the central baryon number density of the PNS PSR J0348+0432 should be in the range $\rho_{c, \text{PNS}} = 0.539 \sim 0.698 \text{ fm}^{-3}$, while that of the NS PSR J0348+0432 is in the wider range $\rho_{c, \text{NS}} = 0.634 \sim 0.859 \text{ fm}^{-3}$.

The field strengths of mesons σ, ω and ρ in the PNS PSR J0348+0432 and those in the NS PSR J0348+0432 make little difference corresponding to a same baryon number density ρ . But the value range of the central field strength of mesons σ, ω and ρ in the PNS PSR J0348+0432 is smaller than those in the NS PSR J0348+0432.

The central chemical potentials of neutrons and electrons in the PNS PSR J0348+0432 are all smaller than those in the NS PSR J0348+0432.

In our calculations baryon octet is considered. we find that inside the NS PSR J0348+0432 only neutrons, protons, Λ and Ξ^- produce. But in the PNS PSR J0348+0432, hyperons $\Sigma^-, \Sigma^0, \Sigma^+$ and Ξ^0 will also produce, though their relative particle number density are very small.

The higher temperature would be advantageous to the production of the hyperons $\Sigma^-, \Sigma^0, \Sigma^+$ and Ξ^0 .

In this work, we consider the PNS as static star and the effects of rotation on PNS are not included. But the research results show that the conservation of baryon number and angular momentum will determine the maximum frequencies of

The property difference between the neutron star PSR J0348+0432 and its proto neutron star 13

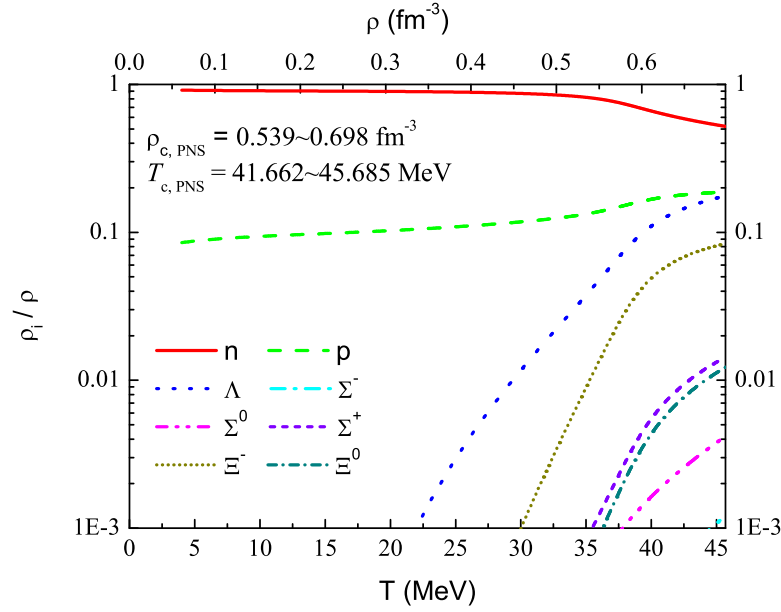


Fig. 7. Effect of temperature on the relative particle number density of the baryons in the PNS PSR J0348+0432.

rotation during the cooling^{30,31}. Therefore, in the next work we should study the effect of rotation on the properties of the PNS PSR J0348+0432.

Acknowledgments

We are thankful to Shan-Gui Zhou for fruitful discussions during my visit to the Institute of Theoretical Physics of Chinese Academy of Sciences. This work was supported by the Natural Science Foundation of China (Grant No. 11447003) and the Scientific Research Foundation of the Higher Education Institutions of Anhui Province, China (Grant No. KJ2014A182).

References

1. A. Burrows, J. M. Lattimer, *Astrophys. J.*, **307**, 178(1986)
2. F. Gulminelli, Ad. R. Raduta, M. Oertel, J. Margueron, *Phys. Rev. C*, **87**, 055809(2013)
3. H. Sawai, S. Yamada, H. Suzuki, *The Astrophysical Journal Letters*, **770**, L19(2013)
4. Ad. R. Raduta, F. Aymard, F. Gulminelli, *The European Physical Journal A*, **50**, 24(2014)
5. G. Camelió, L. Gualtieri, J. A. Pons, V. Ferrari, 2016, eprint arXiv:1601.02945

14 *Xian-Feng Zhao*

6. G.F. Burgio, M. Baldo, O.E. Nicotra, H. J. Schulze, *Astrophys Space Sci.*, **308**, 387(2007)
7. O. E. Nicotra, M. Baldo, G. F. Burgio, H. J. Schulze, *Astronomy and Astrophysics*, **451**, (2006)213
8. P.B.Demorest, T.Pennucci, S.M.Ransom, et al., *Nature* **467**, 1081(2010)
9. J. Antoniadis, P. C. C. Freire, N. Wex, et al., *Science*, **340**, 448(2013)
10. I. Bednarek, P. Haensel, J. L. Zdunik, M. Bejger, R. Maka, *Astronomy & Astrophysics*, **543**, A157(2012)
11. M. Prakash, I.Bombaci, M. Prakash, et al., *Phys. Rep.*, **280**, 1(1997)
12. J. Schaffner et al., *Ann. Phys.*,**235**,35(1994)
13. N.K.Glendenning, *Compact Stars: Nuclear Physics, Particle Physics, and General Relativity*, Springer-Verlag, New York, Inc, 1997.
14. N. K. Glendenning, *Phys. Lett. B*, **185**, 275(1987)
15. N. K. Glendenning, *Nucl. Phys. A*, **469**, 600(1987)
16. M. Reddy, M. Prakash, J. M. Lattimer, *Phys. Rev. D*, **58**, 013009(1998)
17. [R. C. Tolman, *Phys. Rev.*, **55**, 364\(1939\)](#)
18. [J. R. Oppenheimer, G. M. Volkoff, *Phys. Rev.*, **55**, 374\(1939\)](#)
19. N.K. Glendenning, *Ap. J.* **293**,470(1985)
20. J. Schaffner, I. N. Mishustin, *Phys. Rev. C* 53, 1416(1996).
21. C. J. Batty, E. Friedman, A. Gal, *Phys.Rep.* **287(5)**, 385(1997).
22. M. Kohno, Y. Fujiwara, Y. Watanabe, K. Ogata, M. Kawai, *Phys. Rev. C* **74(6)**, 064613(2006).
23. T. Harada, Y. Hirabayashi, *Nucl. Phys. A* **759**, 143(2005).
24. T. Harada, Y. Hirabayashi, *Nucl. Phys. A* **767**, 206(2006).
25. E. Friedman, A. Gal, *Phys.Reports* **452**, 89(2007).
26. J. Schaffner-Bielich, A. Gal, *Phys. Rev. C* **62**, 034311(2000).
27. N. K. Glendenning, S. A. Moszkowski, *Phys.Rev.Lett.* **67**, 2414(1991).
28. X. F. Zhao, *Phys. Rev. C*, **92**, 055802(2015)
29. X. F. Zhao, H. Y. Jia, *Phys. Rev. C*, **85**, 065806(2012)
30. B. Franzon, V. Dexheimer, S. Schramm, *Phys. Rev. D*, **94**, 044018(2016)
31. V. Dexheimer, S. Schramm, *Astrophys. J.*, **683**, 943(2008)